Calculation of the coherent dynamic structure factor of polyisoprene from molecular dynamics simulations

Neil E. Moe and M. D. Ediger
Department of Chemistry, University of Wisconsin, Madison, Wisconsin 53706
(Received 7 August 1998)

The static structure factor $S(Q)$ and the coherent dynamic structure factor $S(Q,t)$ are calculated from molecular dynamics simulations of polyisoprene melts and compared with neutron scattering results [R. Zorn, D. Richter, B. Farago, B. Frick, F. Kremer, U. Kirst, and L. J. Fetters, Physica B **180&181**, 534 (1992)]. Both the shape and the absolute time scale of the calculated $S(Q,t)$ are consistent with experimental results. The decay of $S(Q,t)$ can be almost entirely attributed to *intramolecular* dynamics throughout the Q range studied ($1.2 \leqslant Q \leqslant 3.0$ Å^{-1}), i.e., the full $S(Q,t)$ can be approximated by considering only the self terms and the cross terms localized to within a few repeat units along the chain. It was found that the factor of 5 observed between the dynamics at the first two peaks of $S(Q)$ is part of a general trend largely independent of whether $S(Q)$ is at a minimum or a maximum. A comparison of $S(Q,t)$ in the region of the first peak in $S(Q)$ and the P_2C—H bond vector orientation autocorrelation function $F_C(t)$ suggests that the same molecular motions influence both the neutron spin echo and NMR T_1 relaxation experiments. [S1063-651X(98)12712-5]

PACS number(s): 83.10.Nn, 81.05.Lg, 61.12.Ex, 67.40.Fd

I. INTRODUCTION

A number of different experimental techniques have been used to study local motions in amorphous polymers. NMR T_1 relaxation times depend on the reorientation of individual C—H bond vectors in the polymer [1,2]. Dielectric relaxation measurements follow the reorientation of molecular dipoles [3]. Neutron spin echo techniques are sensitive to local density fluctuations, i.e., the translational motion of the component atoms [4–6]. The coherent dynamic structure factor $S(Q,t)$ measured by neutron spin echo depends on the motion of *each* atom with respect to *every other* atom in the system, including itself. All atomic motions affect this observable whereas pure translational motion does not influence the NMR or the dielectric relaxation experiment.

Many theories and simulations have been used with some success to describe the molecular motions which constitute local polymer dynamics [7–14] and to demonstrate their connection to the NMR T_1 experiment [1,15,16]. The relationship between $S(Q,t)$ and these molecular motions has recently been discussed in the literature. Arbe *et al.* [5] have proposed a simple molecular model which is consistent with their neutron spin echo data on polybutadiene; the same model is also used to describe polyisobutylene data in Ref. [6]. Molecular dynamics simulations can potentially offer new insights: The atomic coordinates contained in the trajectories represent a completely specified classical system which can be used to calculate any experimental observable which depends only upon the time-dependent positions of the atoms. Thus a realistic molecular dynamics trajectory contains a picture of all the molecular motions underlying dielectric relaxation, NMR relaxation, and $S(Q,t)$. The task of classifying the important motions then hinges on the conceptual problem of finding an appropriate way to analyze the atomic coordinates.

Here we use molecular dynamics simulations of polyisoprene melts to study the molecular motions which are responsible for the decay of the coherent dynamic structure factor $S(Q,t)$. This is the first such study on a polymeric system to our knowledge [17]. We also compare $S(Q,t)$ with the correlation function $F_C(t)$ for C—H bond vectors which determines the value of T_1 in a NMR experiment. We begin by describing new simulations of polyisoprene melts at 363 K. This is followed by a description of the calculation of $F_C(t)$, $S(Q,t)$, and the static structure factor $S(Q)$. In Sec. V we compare our simulations with neutron spin echo experiments on polyisoprene by Zorn *et al.* [4]. The shape of the simulated $S(Q,t)$ is consistent with experiment and the simulations accurately reproduce the factor of 5 between the dynamics at the first two peaks in $S(Q)$. This difference need not be attributed to a changeover from an *intramolecular* mechanism to an *intermolecular* one as suggested in Ref. [4] but is rather part of a general trend as a function of Q. In Sec. VI we consider which subset of atomic pairs can account for the decay of $S(Q,t)$. At all Q studied ($1.2 \leqslant Q \leqslant 3.0$ Å^{-1}) $S(Q,t)$ is dominated by atomic pairs localized to within a few repeat units along the polymer chain. In Sec. VII we compare $S(Q,t)$ and $F_C(t)$. The similar time scales of the decay of $S(Q,t)$ and $F_C(t)$ as well as the apparent *intramolecular* character of each suggests that the same molecular motions influence both the NMR and neutron spin echo experiments.

II. SIMULATION DESCRIPTION

We report here atomistic molecular dynamics simulations of polyisoprene melts at 363 K and 1 atm. Each of the four independent cells consisted of a 100-mer of polyisoprene (1302 atoms) with cubic periodic boundary conditions. The polyisoprene used was 100% *cis*-1,4- and had all head-to-tail linkages. Its structure is shown below:

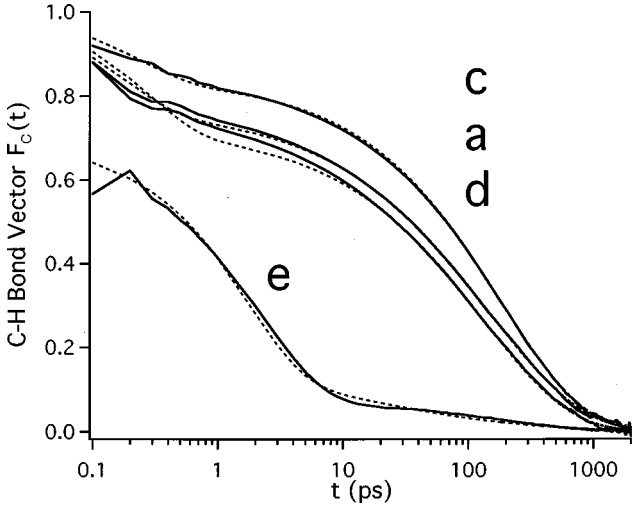

FIG. 1. P_2 orientation autocorrelation functions for C—H bond vectors *a*, *c*, *d*, and *e* calculated from simulations of polyisoprene at 363 K (solid lines). The dashed lines are the fits explained in the text.

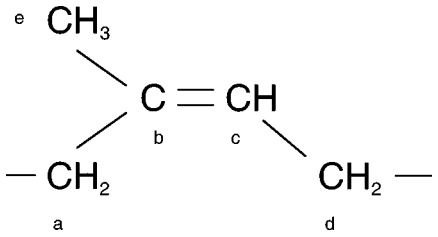

Each of the four initial configurations used in these simula tions was energy-minimized and the configurations were the same ones used previously in generating trajectories at 413 K [18]. In this case we allowed the simulation boxes to equilibrate at 363 K and 1 atm for 1 ns. Afterwards the atomic coordinates were saved at 0.1 ps intervals over a period of 2 ns. Further simulation details may be found in Ref. [18].

III. C—H BOND VECTOR REORIENTATION

NMR experiments are sensitive to the reorientation of vectors fixed in the local molecular frame. For example, ^{13}C T_1 relaxation experiments depend upon $F_C(t)$, the P_2 orientation autocorrelation function for C—H bond vectors:

$$F_C(t)=\langle P_2(\hat{x}(0)\cdot\hat{x}(t))\rangle=\langle 3\cos^2\Theta(t)-1\rangle/2. \quad (1)$$

P_2 is the second Legendre polynomial, $\hat{x}(t)$ is a unit vector in the direction of the C—H bond at time t, and $\Theta(t)$ describes the orientation of the vector at time t relative to its orientation at time 0.

Figure 1 shows the P_2 autocorrelation functions for C—H vectors *a*, *c*, *d*, and *e* calculated from the trajectories at 363 K (a similar plot for 413 K can be found in Fig. 3 in Ref. [18]). We used a fast exponential and a slower stretched exponential to fit the correlation functions for the backbone C—H vectors *a*, *c*, and *d*,

$$F_C(t)=ae^{-t/\tau_1}+(1-a)e^{-(t/\tau_2)^\beta}, \quad (2)$$

TABLE I. Fitting parameters for $F_C(t)$ of backbone C—H bond vectors. Numbers in parentheses are standard deviations comparing trajectories with different starting configurations.

C—H vector	Temperature (K)	a	τ_1 (ps)	τ_2 (ps)	β	τ_c (ps)
a	363	0.23	0.39	148	0.59	175 (64)
a	413	0.21	0.10	56	0.57	71 (29)
c	363	0.16	0.41	184	0.66	208 (74)
c	413	0.14	0.13	70	0.61	89 (36)
d	363	0.28	0.53	133	0.63	136 (44)
d	413	0.26	0.32	50	0.60	56 (16)

where $\tau_1<\tau_2$ and $\beta\leqslant 1$. The fits are shown in Fig. 1 as dashed lines [19]. The orientation correlation time τ_c is the time integral of the correlation function:

$$\tau_c=\int_0^\infty F_C(t)dt. \quad (3)$$

Rapidly decaying correlation functions result in small τ_c's and imply fast dynamics. The fitting parameters and correlation times are compiled in Table I.

IV. CALCULATION OF $S(Q)$ AND $S(Q,t)$

$S(Q)$ can easily be calculated directly from the atomic coordinates, following the prescription in Ref. [20].

$$S(Q)=\frac{1}{N}\sum_{i=1}^{N}\sum_{j=1}^{N}\left[\frac{\sin(Qr_{ij})}{Qr_{ij}}\right]\Delta_{ij}(R) - \frac{4\pi\rho}{Q^2}\left[\frac{1}{Q}\sin QR-R\cos QR\right], \quad (4a)$$

where

$$\Delta_{ij}(R)=\begin{cases}1 & \text{if } r_{ij}\leqslant R\\ 0 & \text{if } r_{ij}>R.\end{cases} \quad (4b)$$

The double sum is taken over each atom in a given frame (irrespective of carbon or hydrogen [21]). If the distance r_{ij} between two atoms is greater than the cutoff distance R (taken to be 12 Å, or about half the simulation cell size) then that pair is not included in the sum. The second term in Eq. (4a) is the analytical solution of the double sum over distances R to ∞ and is exactly correct in the limit that $g(r_{ij}\geqslant R)$ is one, a condition which is approximately fulfilled in these simulations. We calculated $S(Q)$ from a large number of frames throughout the trajectories and took the average [22].

A detailed prescription for calculating $S(Q,t)$ is found in Ref. [20]. Using the atomic coordinates stored in the trajectories, the following function was evaluated:

TABLE II. Density (g/cm^3).

	ρ (363 K)	ρ (413 K)	α (K^{-1})
Simulation	0.798 (0.003)	0.775 (0.002)	5.8×10^{-4}
Experiment [29]	0.869	0.836	6.7×10^{-4}

$$S(Q,t)=\left[\frac{1}{N}\sum_{i=1}^{N}\sum_{j=1}^{N}\left(\frac{\sin(Qr_{ij}(t))}{Qr_{ij}(t)}\right)\Delta_{ij}(R,t) - \frac{4\pi\rho}{Q^2}\left(\frac{1}{Q}\sin QR - R\cos QR\right)\right] \Big/ S(Q,0), \tag{5}$$

where $r_{ij}(t)$ is the distance between atom i at an arbitrary starting time $t=0$ and atom j at some later time t. $\Delta_{ij}(t)$ is evaluated using $r_{ij}(t)$.

We calculated $S(Q,t)$ in increments of 0.3 Å^{-1} over the range $0.9\leqslant Q\leqslant 3.9$ Å^{-1}. This procedure was computationally intensive and took at least as much time as was used to generate the molecular dynamics trajectories. We evaluated $S(Q,t)$ at 300 evenly spaced times t. To achieve adequate averaging the whole calculation was repeated using different starting times $t=0$ (120 starting times at $Q=1.2$, 1.8, 2.1, and 3.0 Å^{-1} and 12 starting times at other Q).

V. COMPARISON OF SIMULATION AND EXPERIMENT

The simulations reproduce many important qualitative features of the neutron scattering measurements. In addition, the absolute time scale for the decay of the simulated $S(Q,t)$ is consistent with an extrapolation of experimental values to higher temperature. Many of the differences between the experiments and simulations may be due to different microstructures (the simulations used 100% *cis*-polyisoprene while the experiments were performed on a sample with 76:18:6 *cis:trans:vinyl* content) and different temperature ranges, as discussed below. The reasonable agreement obtained gives us confidence that the microscopic description of the dynamics extracted from the simulations in Sec. VI is also reasonably realistic.

A. Static properties

Table II compares the density calculated from the simulations with experimental values. Both the density and the thermal expansion coefficient are somewhat low, making complete quantitative agreement with experiment unlikely for other properties. Figure 2 shows $S(Q)$ for polyisoprene obtained from the simulations and the experimental curve from Ref. [4]. Qualitatively, three peaks are found in similar places in each spectrum. However, the simulated spectrum does deviate from experiment in two major respects: (1) the region at $Q<2$ Å^{-1} is shifted to slightly lower Q (the first two peaks occur at 1.2 and 1.8 Å^{-1} in the simulations and 1.44 and 1.92 Å^{-1} in the experiment), and (2) the intensity of the first peak is much greater than the second. The shift to lower Q is likely caused by the simulation density being too low (see Table II) and possibly by the differing microstructures. The difference in density may be augmented by a temperature difference between the simulations and experiments (the temperature is not given in Ref. [4]). The different microstructures are at least partly responsible for the second discrepancy; the enhancement of the first peak seen in the simulations is likely due to more ordered local packing in the 100% *cis* polymer.

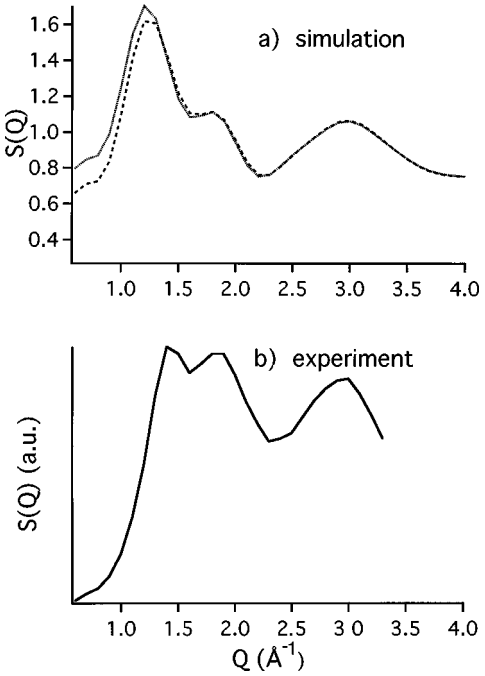

FIG. 2. Static structure factor $S(Q)$ for polyisoprene (a) calculated from the simulations at 363 (---) and 413 K (···) and (b) obtained using neutron scattering by Zorn *et al.* [4].

B. Coherent dynamic structure factor

Temperature differences preclude direct comparison of the molecular dynamics and neutron spin echo results. However, as changes in temperature are not expected to influence the shape of $S(Q,t)$ high above T_g, comparing shapes is a reasonable alternative. Figure 3 contains plots of $S(Q,t)$ calculated from the simulations at the first two peaks of $S(Q)$ ($Q=1.2$ and 1.8 Å^{-1}) at temperatures of 363 and 413 K. Overlaid are the corresponding neutron spin echo curves, $Q=1.44$ and 1.92 Å^{-1}, at 320 K, the highest experimental temperature. The experimental curves have been shifted horizontally along the logarithmic axis in order to give the closest match to the simulation results. The shapes of the simulated curves are reasonably consistent with those of the experimental curves, particularly at $Q=1.2$ Å^{-1}.

In order to make a more quantitative comparison, we fit the correlation functions to the functional form of a fast exponential and a slower stretched exponential [Eq. (2)]. Typical fits are shown in Fig. 3 and pertinent fitting parameters are compared in Table III. In particular, the values of β derived from the simulations are in quite good agreement with experiment.

A convenient quantity defining the absolute time scale of the dynamics is the area under the curve $S(Q,t)$,

$$\tau_{\mathrm{NSE}}=\int_0^\infty S(Q,t)dt. \tag{6}$$

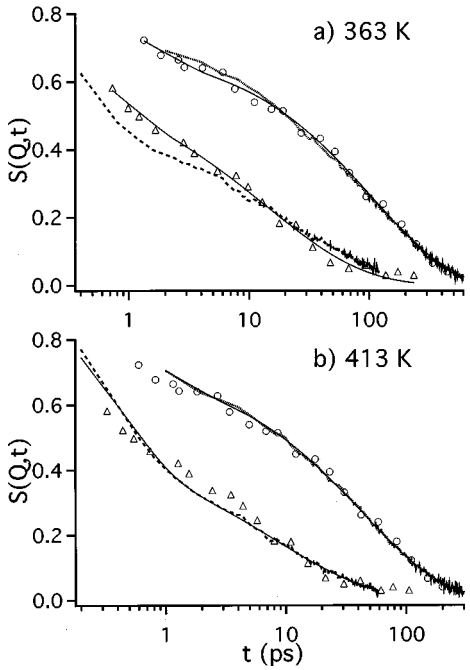

FIG. 3. Dynamic structure factor $S(Q,t)$ for polyisoprene from simulations at $Q=1.2$ (···) and 1.8 Å^{-1} (---). The simulation curves at 1.2 and 1.8 Å^{-1} have been overlaid with the experimental $S(Q,t)$ for 1.44 (circles) and 1.92 Å^{-1} (triangles), respectively [4]. The experimental curves, obtained at 320 K, have been shifted horizontally to compare with simulation results at higher temperature. The solid lines are fits to Eq. (2) for the experiments (a) and the simulations (b).

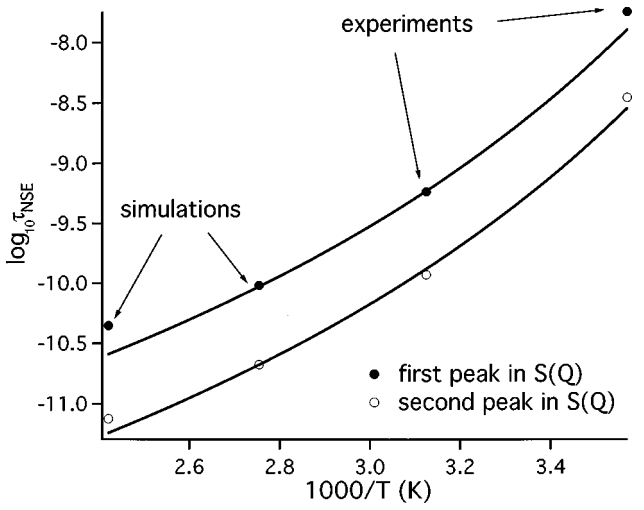

FIG. 4. The logarithm (base 10) of the correlation time τ_{NSE} as a function of temperature at the first two peaks in $S(Q)$ from simulations and neutron spin echo experiments [4]. The solid circles correspond to the first peak at $Q=1.2$ or 1.44 Å^{-1} (simulations and experiments, respectively) and the open circles to the second peak at $Q=1.8$ or 1.92 Å^{-1} (simulations and experiments). The results at the two higher temperatures are from the simulations and at the lower temperatures are from the experiments. The solid lines show the VFT temperature dependence given in Ref. [4]. The dynamics in the simulation occur on a time scale which is consistent with experimental results, considering the temperature difference. The factor of 5 observed between the dynamics at the first two peaks of $S(Q)$ is also well reproduced.

The values of τ_{NSE} and the fitting parameters obtained using Eq. (2) for the simulated $S(Q,t)$ at $Q=1.2$, 1.8, 2.1, and 3.0 Å^{-1} are listed in Table IV.

Figure 4 shows $\log_{10}(\tau_{NSE})$ from the simulations and neutron spin echo experiments [4,23] at the first two peaks in $S(Q)$ as a function of $1000/T$. The solid lines are the temperature dependence of the viscosity, which was shown in Ref. [4] to be similar to the temperature dependence of the experimental results over the range 230–320 K (only the two highest experimental temperatures are shown in Fig. 4). The simulation results are consistent with an extrapolation of the experimental values to higher temperature, although the near perfect correspondence is surely fortuitous given that the simulation density is too low. The simulations correctly reproduce the factor of 5 between the dynamics at the first two peaks in $S(Q)$ reported in Ref. [4].

Figure 5 shows $\log_{10}(\tau_{NSE})$ as a function of $\log_{10}Q$ calculated from the simulations at 363 and 413 K. Reasonable linear fits are given, with slopes of -4.4 and -4.2, respectively. The factor of 5 difference observed between τ_{NSE} at $Q=1.2$ and 1.8 Å^{-1} is part of a general trend. Within this Q range, if Q changes by 50%, then τ_{NSE} changes by roughly a factor of 5 independent of Q [24].

TABLE III. Comparison of shape of $S(Q,t)$.

	Q (Å^{-1})	a	β
Simulation at 413 K	1.2	0.28	0.65
Simulation at 363 K	1.2	0.28	0.66
Experiment at 320 K	1.44	0.30	0.67
Simulation at 413 K	1.8	0.50	0.54
Simulation at 363 K	1.8	0.48	0.51
Experiment at 320 K	1.92	0.40	0.57

VI. HOW LOCALIZED ARE THE MOTIONS WHICH DETERMINE $S(Q,t)$?

The full range of motions which contribute to the decay of the coherent dynamic structure factor $S(Q,t)$ are extremely complex, as can be inferred from Eq. (5). Although in principle $S(Q,t)$ depends on the translational motion of *each* atom with respect to *every other* atom (including itself) in the system, not every term makes a significant contribution to the sum. For example, the net contribution to $S(Q,t)$ from all pairs of atoms with separation r_{ij} large enough so that $g(r_{ij})=1$ will be exactly zero. This corresponds to a distance of about 1 nm in many amorphous systems. In the subnanometer regime, motions involving greater atomic displacements will be required to produce a given change in $S(Q,t)$ as Q decreases. Thus $S(Q,t)$ at low Q decays more slowly than at higher Q and may also depend on atomic pairs with larger r_{ij}.

A. Isolation of intramolecular contributions to $S(Q,t)$

We isolated small subsets of terms from Eq. (5) in order to learn which atomic pairs were most important. We chose to evaluate three different subsets which progressively incorporate more and more atomic pairs over a wider range of

TABLE IV. Fitting parameters for $S(Q,t)$. Numbers in parentheses are standard deviations comparing trajectories with different starting configurations.

Q (Å^{-1})	Temperature (K)	a	τ_1 (ps)	τ_2 (ps)	β	τ_{NSE} (ps)
1.2	363	0.28	0.57	99.0	0.66	95.9 (50)
1.2	413	0.28	0.54	44.7	0.65	44.2 (14)
1.8	363	0.48	0.37	20.5	0.51	21.1 (10)
1.8	413	0.50	0.42	8.32	0.54	7.53 (1.7)
2.1	363	0.63	0.33	14.8	0.53	10.1 (1.0)
2.1	413	0.71	0.33	7.18	0.64	3.02 (0.5)
3.0	363	0.83	0.24	6.13	0.42	3.35 (1.1)
3.0	413	0.86	0.23	2.94	0.49	1.03 (0.1)

distances $r_{ij}(0)$. Comparison of these partial dynamic structure factors $S_{\text{partial}}(Q,t)$ to the full $S(Q,t)$ calculated using all the atomic pairs within 12 Å determines the relative importance of each subset.

The subset for which $r_{ij}(0)$ is smallest is when $i=j$, i.e., the initial atomic separation is 0. These self terms were grouped in $S_{\text{self}}(Q,t)$, which is similar to the incoherent dynamic structure factor. We also evaluated a subset $S_{1\text{RU}}(Q,t)$ where i and j were constrained to be part of the same repeat unit (as defined by the structure above). The last partition, $S_{5\text{RU}}(Q,t)$, included terms for which i and j were part of the same repeat unit or within ± 2 repeat units along the chain. We claim below that $S_{5\text{RU}}(Q,t)$ is nearly equivalent to the single-chain dynamic structure factor in the melt and contains most of the *intramolecular* contributions to $S(Q,t)$.

The correct way to calculate the *intramolecular* subsets $S_{\text{partial}}(Q,t)$ from the trajectory is to turn off the periodic boundary conditions and to evaluate a modified version of Eq. (5):

$$S_{\text{partial}}(Q,t)=\left[\frac{1}{N}\sum_{i=1}^{N}\sum_{j=x}^{y}\left(\frac{\sin(Qr_{ij}(t))}{Qr_{ij}(t)}\right)\right]\Big/\, S(Q,0). \tag{7}$$

The values of x and y are determined by the particular subset

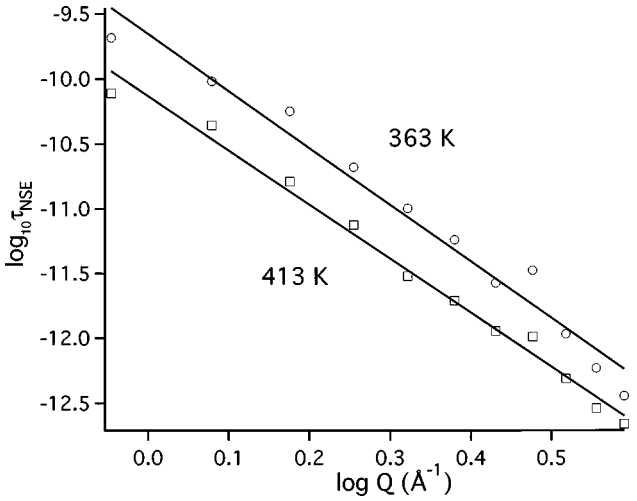

FIG. 5. $\log_{10}\tau_{\text{NSE}}$ versus $\log_{10}Q$ calculated from the simulations at 363 (circles) and 413 K (squares). The solid lines are linear fits which approximately describe the results over the whole range of Q.

under consideration. The results of these calculations are shown in Fig. 6 for $Q=1.2$, 1.8, 2.1, and 3.0 Å^{-1} at 363 K (similar results were obtained at 413 K). Each function, the total $S(Q,t)$, $S_{\text{self}}(Q,t)$, $S_{1\text{RU}}(Q,t)$, and $S_{5\text{RU}}(Q,t)$, has been normalized by $S(Q,0)$.

$S_{\text{self}}(Q,t)$. Figure 6 clearly demonstrates the major importance of the self terms in Eq. (5). Even at the lowest Q, these few terms, amounting to only 0.1% of all possible pairs in these simulations, count for a significant portion of the total $S(Q,t)$. This is expected at $t=0$ since the function $\sin[Qr_{ij}(t)]/Qr_{ij}(t)$ is 1.0 for the self terms $i=j$ and is guaranteed to remain positive until the atoms have moved a distance π/Q. No other terms have this unique property at all Q. For an arbitrary pair of atoms, $\sin[Qr_{ij}(t)]/Qr_{ij}(t)$ can be positive or negative and the net effect on $S(Q,t)$ of summing over all pairs is largely one of mutual cancellation. Only at $Q=1.2$ Å^{-1} does $S_{\text{self}}(Q,t)$ fall far short of the total $S(Q,t)$.

$S_{1\text{RU}}(Q,t)$. Figure 6 shows that the self terms and the *intramolecular* cross terms within a single repeat unit of polyisoprene can largely account for the dynamic structure factor at all Q investigated, including $Q=1.2$ Å^{-1}. For $Q=1.2$ Å^{-1}, in addition to the self terms included in $S_{1\text{RU}}(Q,t)$, pairs of directly bonded atoms $[r_{ij}(0)=1.1\text{–}1.6\ \text{Å}]$ are guaranteed to contribute positively $(\sin[1.2r_{ij}(0)]/1.2r_{ij}(0)=0.5\text{–}0.75)$. This high proportion of positive terms causes the initial value of $S_{1\text{RU}}(1.2,0)$ to be greater than that of the total dynamic structure factor $S(1.2,0)$. Since $S_{1\text{RU}}(Q,t)$ and $S_{\text{self}}(Q,t)$ at higher Q are identical, the cross terms which contribute to $S_{1\text{RU}}(Q,t)$ in these cases must sum to zero.

$S_{5\text{RU}}(Q,t)$. As we included more and more terms for pairs of atoms farther and farther away along the chain contour, we soon reached a limit where the additional cross terms had little effect on the partial dynamic structure factor. An analogous calculation, $S_{7\text{RU}}(Q,t)$ (not shown), gave very similar results to $S_{5\text{RU}}(Q,t)$ in Fig. 6. This suggests that $S_{5\text{RU}}(Q,t)$ is a good approximation to the *intramolecular* contribution to $S(Q,t)$. The small difference observed between $S_{5\text{RU}}(Q,t)$ and $S(Q,t)$ approximates the *intermolecular* contribution to the dynamic structure factor [25]:

$$S(Q,t)\cong S_{5\text{RU}}(Q,t)+S_{\text{inter}}(Q,t). \tag{8}$$

Even at $Q=1.2$ Å^{-1}, $S(Q,t)$ is almost completely an *intramolecular* function.

We fit the partial dynamic structure factors to a functional form similar to Eq. (2),

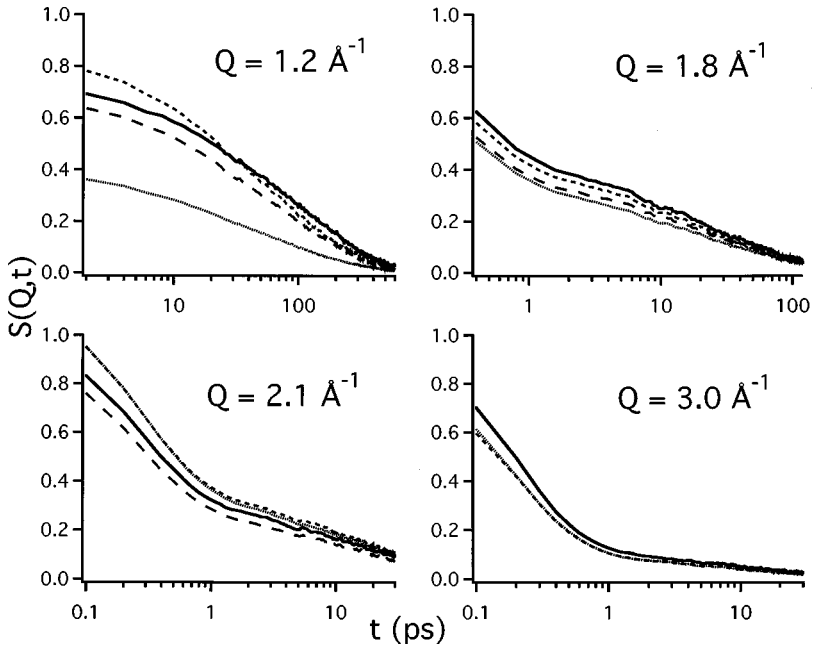

FIG. 6. $S(Q,t)$ and the various partial dynamic structure factors $S_{\text{partial}}(Q,t)$ for $Q=1.2$, 1.8, 2.1, and 3.0 Å^{-1} calculated from the simulations at 363 K. The full $S(Q,t)$ (———), $S_{5\text{RU}}(Q,t)$ (– – –), $S_{1\text{RU}}(Q,t)$ (---), and $S_{\text{self}}(Q,t)$ (···) are shown. The self terms $S_{\text{self}}(Q,t)$ account for the major portion of $S(Q,t)$ at all but the lowest value of Q. The addition of cross terms within the same repeat unit yielding $S_{1\text{RU}}(Q,t)$ is enough to account for the major portion of $S(Q,t)$, even at 1.2 Å^{-1}. Thus *intramolecular* terms in Eq. (5) largely determine $S(Q,t)$ over the range of Q studied.

$$S_{\text{partial}}(Q,t)=ae^{-t/\tau_1}+(b-a)e^{-(t/\tau_2)^{\beta}}, \tag{9}$$

where b is the value of the function at $t=0$ and is in general not equal to one. The values of b are compiled in Table V. The relaxation time τ_{partial} is defined as

$$\tau_{\text{partial}}=\int_{t=0}^{\infty} S_{\text{partial}}(Q,t)dt. \tag{10}$$

Figure 7 plots the ratio $\tau_{\text{partial}}/\tau_{\text{NSE}}$ as a function of Q and temperature. This ratio clearly increases as temperature is lowered at the peaks in the static structure factor ($Q=1.2$,1.8,3.0 Å^{-1}). This suggests that the *intramolecular* terms will dominate $S(Q,t)$ to an even greater extent in experiments performed at lower temperatures. At $Q=2.1$ Å^{-1} this trend is apparently reversed, which is likely related to the fact that $S(Q)$ is at a minimum rather than a maximum.

B. Role of intermolecular correlations

The analysis above indicates that a small *intramolecular* subset of terms from Eq. (5) almost completely accounts for the decay of $S(Q,t)$. We have not tested the hypothesis that a subset of *intermolecular* terms can account for the decay of $S(Q,t)$ for at least some Q. It is probable that some groups of mostly positive cross terms can be chosen which approximately reproduce the full $S(Q,t)$. However, the appropriate subset of cross terms would likely be dependent on Q. It is unlikely that any subset of *intermolecular* terms would be able to match the full $S(Q,t)$ over the whole Q range to the remarkable extent observed with the *intramolecular* subsets $S_{1\text{RU}}(Q,t)$ and $S_{5\text{RU}}(Q,t)$.

Physically, one does expect significant coupling between intramolecular and intermolecular motions in polyisoprene melts. Certainly the motion of a polymer chain segment is greatly restricted by the presence of neighboring chains. However, these simulations indicate that the influence of neighboring chains on $S(Q,t)$ is largely indirect; the explicit effect of atoms on neighboring chains on the full $S(Q,t)$ at

TABLE V. Initial value of $S_{\text{partial}}(Q,t=0)$.

	Temperature (K)	$Q=1.2$ Å^{-1}	$Q=1.8$ Å^{-1}	$Q=2.1$ Å^{-1}	$Q=3.0$ Å^{-1}
$S_{\text{self}}(Q,t)$	363	0.62	0.90	1.20	0.94
	413	0.59	0.88	1.23	0.94
$S_{1\text{ru}}(Q,t)$	363	1.21	0.98	1.15	0.87
	413	1.16	0.99	1.17	0.87
$S_{5\text{ru}}(Q,t)$	363	0.98	0.88	0.93	1.00
	413	0.94	0.90	0.95	1.00

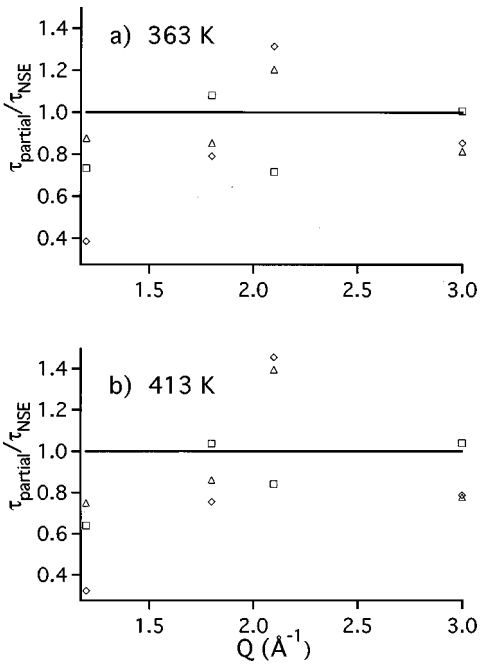

FIG. 7. Plots of τ_{self} (diamonds), τ_{1RU} (triangles), and τ_{5RU} (squares) normalized by τ_{NSE} at $Q=1.2$, 1.8, 2.1, and 3.0 Å^{-1} calculated from the simulations at (a) 363 and (b) 413 K. At peaks in $S(Q)$ ($Q=1.2$, 1.8, and 3.0 Å^{-1}), *intramolecular* terms in Eq. (5) become more important as temperature decreases, while the opposite trend is apparent near the minimum in $S(Q)$ ($Q=2.1$ Å^{-1}).

$Q=1.2$ Å^{-1} is estimated to be 25–35 % from comparing the integrals of $S_{5RU}(Q,t)$ and $S(Q,t)$ in Fig. 7. The most important intermolecular cross terms likely involve atoms on repeat units which are adjacent to each other.

C. Implications for interpreting experimental results for polyisoprene

In Ref. [4] Zorn *et al.* suggest that the difference in the rate of decay of $S(Q,t)$ for polyisoprene at $Q=1.44$ and 1.92 Å^{-1} is due to a change in the mechanism of the dynamics, that $S(Q,t)$ is an *intramolecular* function at high Q and an *intermolecular* function at low Q. This is inconsistent with our analysis in the preceding section. In addition, in Fig. 5 we show that τ_{NSE} varies with Q in a similar way throughout the range $0.9 \leqslant Q \leqslant 3.9$ Å^{-1}. This too suggests that it is unnecessary to invoke any change in mechanism. An approximately linear relationship between $\log_{10}$ (relaxation time) and $\log_{10}Q$ was also observed for polybutadiene and polyisobutylene in Refs. [5,6].

VII. COMPARISON OF $S(Q,t)$ AND THE NMR $F_C(t)$

As shown in Eqs. (1) and (5), very different calculations are required to obtain the experimental observables for the NMR T_1 relaxation and neutron spin echo experiments: The reorientation of C—H bond vectors determines T_1 while local density fluctuations determine $S(Q,t)$. Yet both the neutron spin echo [4–6] and NMR [26,27] observables have been shown experimentally to follow the temperature dependence of the α relaxation in some polymers. These simulations offer further evidence that the same fundamental motions influence both experiments in polyisoprene.

A comparison of Tables I and IV indicates that the coherent dynamic structure factor at the first peak in $S(Q)$ ($Q=1.2$ Å^{-1}) is remarkably similar to the P_2 autocorrelation functions for backbone C—H bond vectors; the similarity includes not only the absolute time scales of the decay of these functions, but also their shapes. In addition, τ_{NSE} has nearly the same temperature dependence as τ_c for C—H bond vectors [28].

We have shown in previous work that the structural adjustments which accompany the reorientation of a C—H bond are largely localized to a single repeat unit in polyisoprene (see Fig. 8 in Ref. [15]). This result is comparable to our observation in this work that the coherent dynamic structure factor in the region between $Q=1.2$ and 3.0 Å^{-1} can be directly calculated considering only the atoms within one, or at most a few repeat units along the chain. The apparent shared *intramolecular* character of $S(Q,t)$ and $F_C(t)$ as well as comparable relaxation rates suggests that they reflect the same molecular dynamics.

VIII. CONCLUSIONS

We have calculated the static structure factor $S(Q)$ and the coherent dynamic structure factor $S(Q,t)$ for polyisoprene from molecular dynamics simulations. Comparison with neutron spin echo results shows that the dynamics seen in the simulations are reasonably realistic. A plot of the log of the integral of $S(Q,t)$, $\log_{10}\tau_{NSE}$, versus $\log_{10}Q$ was approximately linear, nearly independent of fluctuations in $S(Q)$. While the full $S(Q,t)$ depends on all the atomic coordinates, we found that this function could be reasonably approximated at all Q studied by including only *intramolecular* atomic pairs for which the separation was very small. Of course $S(Q,t)$ is influenced by surrounding chains, but their influence is largely indirect in that they constrain the motion of a given chain.

Our picture differs from the one developed by Arbe *et al.* [5] and Richter *et al.* [6] to explain their experimental results on polybutadiene and polyisobutylene. They calculated $S(Q,t)$ using a model of a hopping process which was consistent with their data at short times. The model then predicted that this *intramolecular* relaxation would be most prominent at higher Q. It was proposed that a slower, *intermolecular* mechanism dominates $S(Q,t)$ at lower Q, near the first peak in the static structure factor. The motivation for their model derives from a physical picture ascribed to the viscoelastic α and β relaxations (associated with *intermolecular* and *intramolecular* processes, respectively) in polymers, which are assumed to underlie $S(Q,t)$.

Our approach to understanding $S(Q,t)$ arose naturally from calculating the function via Eq. (5) from simulation trajectories. We asked the question, ''How many of the terms are necessary to approximate the full function?'' Our conclusion that the *intramolecular* terms within a few repeat units of each other can largely account for the full $S(Q,t)$ is model independent. However, as we argued in Sec. VI, the indirect influence of neighboring chains on $S(Q,t)$ is great. For example, the presence of these neighboring chains leads to the difference in the dynamics between a chain in a dense melt and an isolated chain in vacuum, even if in both cases

$S(Q,t)$ could be closely approximated by considering localized *intramolecular* terms.

Our results also point to an underlying similarity between the NMR T_1 experiment and $S(Q,t)$ in this Q range. Analysis of simulation results on polyisoprene in Ref. [15] showed that the reorientation of C—H bond vectors is a very localized process. For example, conformational transitions had very little influence on the reorientation of C—H bond vectors only one repeat unit away from the transition. Both $S(Q,t)$ and the P_2 autocorrelation function for C—H vectors decay on similar time scales. Further work is needed to show how specific molecular motions such as librations and conformational transitions influence $S(Q,t)$.

ACKNOWLEDGMENTS

This project was supported by the National Science Foundation (Grant No. DMR-9732483). The computers used for this work were purchased through a grant from the NSF Chemistry Division (Grant No. CHE-9522057). We acknowledge helpful discussions with Dr. Chwen-Yang Shew and Professor U. Buchenau.

[1] R. Dejean de la Batie, F. Lauprêtre, and L. Monnerie, Macromolecules **22**, 122 (1989).
[2] W. Zhu and M. D. Ediger, Macromolecules **30**, 1205 (1997).
[3] N. G. McCrum, B. E. Reed, and G. Williams, *Anelastic and Dielectric Effects in Polymer Solids* (Wiley, London, 1967).
[4] R. Zorn, D. Richter, B. Farago, B. Frick, F. Kremer, U. Kirst, and L. J. Fetters, Physica B **180&181**, 534 (1992).
[5] A. Arbe, D. Richter, J. Colmenero, and B. Farago, Phys. Rev. E **54**, 3853 (1996).
[6] D. Richter, A. Arbe, J. Colmenero, M. Monkenbusch, B. Farago, and R. Faust, Macromolecules **31**, 1133 (1998).
[7] E. Helfand, Science **226**, 647 (1984).
[8] W. Gronski, Makromol. Chem. **178**, 2949 (1977).
[9] G. Moro, J. Chem. Phys. **97**, 5749 (1992).
[10] A. Perico, Acc. Chem. Res. **22**, 336 (1989).
[11] E.-G. Kim and W. L. Mattice, J. Phys. Chem. **101**, 6242 (1994).
[12] R. H. Gee and R. H. Boyd, J. Chem. Phys. **101**, 8028 (1994).
[13] R.-J. Roe, J. Chem. Phys. **100**, 1610 (1994).
[14] G. D. Smith, D. Y. Yoon, W. Zhu, and M. D. Ediger, Macromolecules **27**, 5563 (1994).
[15] N. E. Moe and M. D. Ediger, Macromolecules **29**, 5484 (1996).
[16] C. Baysal, B. Erman, I. Bahar, F. Lauprêtre, and L. Monnerie, Macromolecules **30**, 2058 (1997).
[17] Smith and co-workers have used molecular dynamics simulations of polyethylene melts to study the incoherent dynamic structure factor $S_{\mathrm{ic}}(Q,t)$: G. D. Smith, W. Paul, D. Y. Yoon, A. Zirkel, J. Hendricks, D. Richter, and H. Schober, J. Chem. Phys. **107**, 4751 (1997); W. Paul, G. D. Smith, D. Y. Yoon, B. Farago, S. Rathgeber, A. Zirkel, L. Willner, and D. Richter, Phys. Rev. Lett. **80**, 2346 (1998).
[18] N. E. Moe and M. D. Ediger, Polymer **37**, 1787 (1996).
[19] The methyl C—H vector e was not well described by Eq. (2), presumably because of the fast rotation about the C—C axis. We fit this correlation function with a sum of two exponentials and a stretched exponential, $F_C(t)=ae^{-t/\tau_1}+be^{-t/\tau_2}+(1-a-b)e^{-(t/\tau_3)^{\beta}}$. The parameters obtained for 363 and 413 K, respectively, are $a=0.23$, 0.37; $\tau_1=0.012$, 0.021 ps; $b=0.46$, 0.45; $\tau_2=1.77$, 1.62 ps; $\tau_3=3.85$, 5.62 ps; $\beta=0.25$, 0.28; $\tau_c=30$, 14 ps.
[20] J. J. Salacuse, A. R. Denton, and P. A. Egelstaff, Phys. Rev. E **53**, 2382 (1996); J. J. Salacuse, A. R. Denton, P. A. Egelstaff, M. Tau, and L. Reatto, *ibid.* **53**, 2390 (1996).
[21] The experiments in Ref. [4] were performed on fully deuterated samples in order to obtain coherent scattering. The coherent scattering lengths of ^{2}H and ^{12}C are almost identical, justifying the approximation used here.
[22] We also calculated finite-size corrections to $S(Q)$ and $S(Q,t)$ using the procedure outlined in Ref. [20]. These effects were small in the Q range we studied, so the results were not incorporated into this paper.
[23] These values were extracted from Ref. [4]. The correlation times at 320 K were taken as the product of $\langle\tau\rangle$ from Fig. 4 and f^0 from Fig. 2 ($f^0=0.811$ and 0.856 at $Q=1.44$ and 1.92 Å^{-1}, respectively). τ_{NSE} at 280 K was then calculated using the temperature dependence shown in Fig. 3. The correlation times were not taken directly from Fig. 3 due to an apparent error in that figure.
[24] Although the trend is approximately linear, the deviations seen are usually in the direction expected for de Gennes narrowing [P. G. de Gennes, Physica (Amsterdam) **25**, 825 (1959)]. We observe that the relaxation times near maxima in $S(Q)$ generally lie above the line while near minima the relaxation times tend to be below the line.
[25] In these single-chain simulations we take *intermolecular* to refer to the cross terms between atoms on repeat units far away along the chain contour. We believe that $S_{5\mathrm{RU}}(Q,t)$ is similar to the single-chain $S(Q,t)$ which could be calculated from a much larger, many-chain simulation.
[26] U. Pschorn, E. Rössler, H. Silescu, S. Kaufmann, D. Shaefer, and H. W. Spiess, Macromolecules **24**, 398 (1991).
[27] D. Schaefer, H. W. Spiess, U. W. Suter, and W. W. Fleming, Macromolecules **23**, 3431 (1990).
[28] In contrast, the temperature dependence for conformational transitions is much lower (the ratio of average conformational transition times at 363 and 413 K is 1.4 compared with values of 2.2–2.5 for τ_{NSE} and τ_c).
[29] *Polymer Handbook*, edited by J. Brandrup and E. H. Immergut (Wiley, New York, 1975).